CrystEngComm

Accepted Manuscript

ROYAL SOCIETY OF CHEMISTRY

www.rsc.org/crystengcomm

Enhanced Photocatalytic Degradation Activity for Tetracycline under Visible Light Irradiation of $Ag/Bi_{3.84}W_{0.16}O_{6.24}$ Nanooctahedrons

Xinying Li[1,2], Liping Wang[2], Dongbo Xu[1], Jincheng Lin[3], Ping Li[1], Shuang Lin[1], Weidong Shi[1]*

Abstract

In this work, $Ag/Bi_{3.84}W_{0.16}O_{6.24}$ nanooctahedrons composite photocatalyst was successfully synthesized by a green method at room temperature using silver nitrate ($AgNO_3$) as silver source. Furthermore, the photocatalytic degradation of TC under visible-light was conducted to investigate the effect of Ag. In particular, the $Ag/Bi_{3.84}W_{0.16}O_{6.24}$ nanooctahedrons composite photocatalyst shown the highest potocatalytic activity when the content of Ag was 10% (the mole ratio R = 0.1). Electron spin resonance examination confirmed the photoinduced active species (•OH and O_2•–) were involved in the photocatalytic degradation of TC. The high efficiency photocatalytic activity of the as-prepared $Ag/Bi_{3.84}W_{0.16}O_{6.24}$ photocatalyst could be ascribed the SPR absorption of silver nanoparticles as well as fast generation, separation and transportation of the photogenerated carriers.

Introduction

Tetracycline (TC), due to its highly effective, bioactive substances, is one of the primarily antibiotics groups used for veterinary purposes, for human therapy and for agricultural purposes. After medication, more than 70 % of tetracycline antibiotics are excreted and released in active form into the environment via urine and feces from humans and animals. TC is broad spectrum antibiotics,

([1]School of Chemistry and Chemical Engineering, Jiangsu University, Zhenjiang, 212013, P. R. China. E-mail: swd1978@ujs.edu.cn; Fax: +86 511 88791108; Tel: +86 511 8879 0187)

([2]School of Environmental and Safety Engineering, Changzhou University, Changzhou, 213164, P. R. China)

([3]Shool of Hydraulic and Environmental Engineering, China Three Gorges University, Yichang, 443002, P. R. China)

and exhibits antibiotic activity against infections caused by both Gram (+) and Gram (-) microorganisms as well as mycoplasma, chlamydia, rickettsiae and protozoan parasites. Unfortunately the degradation of TC cannot be accomplished in the natural environment or biological treatment plants[1-6]. Photocatalytic degradation is a promising method due to its extremely efficient degradation rate, high mineralization efficiency and low toxigenicity, ideally producing CO_2 and H_2O as end products, thus provides a good tool for the transformation and degradation of TC[7-10]. In recent years, the use of UV light irradiations for the degradation of tetracycline antibiotics is one of the approaches that have been widely investigated. The photocatalysis TiO_2 is one AOPS （advanced oxidation processes）of special interest due to the chemical stability of the photocatalyst, low cost, and ability of using the small percentage of the ultraviolet radiation coming from the sun, which may also greatly reduce the operation costs. However, the ultraviolet region accounts for merely about 4% of the incoming solar energy, which makes the efficiently practical application of photocatalytic oxidation in TC treatment as an impossible[11-13]. Therefore, much effort has been made on developing visible-light-driven photocatalysts.

As one of the simplest Aurivillius oxides, bismuth tungstate (Bi_2WO_6) has received much attention due to its good photocatalytic performance in organic contaminant degradation under visible light irradiation[14-16]. In the synthetic process of Bi_2WO_6, a special $Bi_{3.84}W_{0.16}O_{6.24}$ crystal could be found [17-20]. Its formation can be possibly attributed to the different solubility of $WO4^{2-}$and $(Bi_2O_2)^{2+}$ in precursor suspensions with various pH[21]. Zhu et al. ported the photocatalytic degradation of bisphenol-A by $Bi_{3.84}W_{0.16}O_{6.24}$ photocatalysts under simulated solar light irradiation[22], which sufficiently demonstrates the potential of $Bi_{3.84}W_{0.16}O_{6.24}$ for the applications in the photocatalytic degradation of environmental pollutants. In our previous report, we have successfully

synthesized $Bi_{3.84}W_{0.16}O_{6.24}$ nanooctahedrons by a facile inorganic salt-assisted hydrothermal method[23]. But, a slow electron transfer greatly limited the extended applications in photocatalysis. Compared with a single photocatalyst, composite photocatalysts usually exhixibit a high photocatalytic performance for the decomposition of organic contaminants. In general, a heterostructure architecture with short distance between photocarrier generation junction and redox reaction center can reduce the necessary charge diffusion length and effectively reduce the bulk recombination and improve the overall efficiency. Such as metal/semiconductor ($Pt/AgInS_2$,[24] Cu/CuO,[25] $Pd/NaTaO_3$[26]), semiconductor/semiconductor (Ag_2O/Bi_2WO_6,[27] Bi_2O_3/Bi_2WO_6,[28] CuO/In_2O_3[29]), molecule/semiconductor (Ru/TiO_2[30]), and even conjugated polymer/nanocrystal composites (PPV/TiO_2[31]). The surface plasmon resonance (SPR), one of the metal-semiconductor heterostructure architecture, has offered a new opportunity to overcome the limited efficiency of photocatalysts[32.] Plasmonic metallic nanostructures are characterized by their strong interaction with resonant photons through an excitation of surface plasmon resonance. The formation of SPR can not only absorb visible light and convert it to the formation of free energetic electrons, but also promote the electron–hole pair formation rate driven by the electromagnetic field formed nearby the semiconductor.[33] Ag is well-known for its intense interactions with visible-light via the resonance of the oscillations of the free electrons within the particles, and is considered as a relatively cheap noble metal.[34] Various Ag composite photocatalysts, such as Ag/TiO_2, [35]$Ag/AgCl$,[36] Ag/ZnO,[37] Ag/C_3N_4,[38] α/β-$Bi_2O_3/Ag/AgCl$,[39] confirmed Ag can realize efficient separation of photogenerated charge carriers**,** respect to efficient utilization of energy. However, to best of our knowledge there is no report on $Ag/Bi_{3.84}W_{0.16}O_{6.24}$ as a photocatalyst.

In this study, for the first time, $Ag/Bi_{3.84}W_{0.16}O_{6.24}$ composite photocatalyst was synthesized and

its photocatalytic activity was studied. The photoactivity evaluation via the photocatalytic degradation of TC under visible-light irradiation, when the content of Ag was 10% (mole ratio R = 0.1), Ag/$Bi_{3.84}W_{0.16}O_{6.24}$ composite photocatalyst (71.64%) shown higher activity of photocatalytic degradation of TC than pure $Bi_{3.84}W_{0.16}O_{6.24}$ octahedrons (34.39%). Furthermore, the mechanism of the enhanced photocatalytic activity of the Ag/$Bi_{3.84}W_{0.16}O_{6.24}$ composite plasmonic photocatalyst for the degradation of TC solution was also analyzed.

2. EXPERIMENTS

2.1. Synthesis of Ag/$Bi_{3.84}W_{0.16}O_{6.24}$

$Bi_{3.84}W_{0.16}O_{6.24}$ nanostructures were synthesized via a versatile and facile microwave method. A mixture of $Bi(NO_3)_3 \cdot 5H_2O$ (1.0 mmol) and $Na_2WO_4 \cdot 2H_2O$ (0.5 mmol) in 50 mL of deionized water, followed by addition of 2 ml of ethylenediamine (En, 99%). After being stirred for 30 min, the mixture was transferred into a 250 mL round-bottom flask in a microwave system (XH-300UL, Beijing Xiang Hu Technology Development Co. Ltd) equipped within situ magnetic stirring. After treating the mixtureat100 ℃ for 5 min under microwave radiation, The final products were collected by centrifugation, washed several times with deionized water and ethanol, and dried in air at 60 ℃ for 12 h.

Ag/$Bi_{3.84}W_{0.16}O_{6.24}$ nanooctahedrons copisite photocatalyst was prepared by a photo-reduction process as follows: the obtained $Bi_{3.84}W_{0.16}O_{6.24}$ (0.2 mmol) was added into 100 mL $AgNO_3$ solution by magnetic stirring. Photo-reduction was carried out under a 300 W Xe lamp for 1 h during which silver ions are reduced to form silver nanoparticles on the surface of $Bi_{3.84}W_{0.16}O_{6.24}$. The obtained Ag/$Bi_{3.84}W_{0.16}O_{6.24}$ nanooctahedrons was then washed with deionized water, and dried in an oven at

60 °C for 12 h. The molar ratios of Ag to $Bi_{3.84}W_{0.16}O_{6.24}$ (designated as R) were 0.05, 0.1, 0.15 and 0.3.

2.2. Characterization.

The crystal structure of samples was determined by the X-ray diffraction (XRD) method using Cu Kα radiation (λ = 1.54178 Å). The chemical composition of the samples was determined by scanning electron microscope-X-ray energy dispersion spectra (SEM-EDX) with an accelerating voltage of 25 KV. Scanning electron microscopy (SEM) images were collected on an S-4800 field emission SEM (SEM, Hitachi, Japan). Transmission electron microscopy (TEM) and high resolution transmission electron microscopy (HRTEM) images were collected on an F20S-TWIN electron microscope (Tecnai G2, FEI Co.), using a 200 KV accelerating voltage. The investigation of the surface of the sample was by an X-ray photoelectron spectrometer (XPS, PHI-5300). UV-vis diffused reflectance spectra of the samples were obtained from a UV-vis spectrophotometer (UV2550, Shimadzu, Japan); $BaSO_4$ was used as a reflectance standard. The photoluminescence properties of the obtained samples were measured on a Perkin-Elmer LS 55 luminescence spectrometer. The photoluminescence (PL) spectra of sample were conducted on a Perkin-Elmer LS 55 at room temperature using a fluorescence spectrophotometer. ESR analysis was conductedwith a Bruker EPR A300-10/12 spectrometer.

2.3. Photocatalytic Degradation of TC

The photodegradative reaction for Tetracycline （TC） was carried out under simulated sunlight irradiation by using a 150 W Xe lamp with a cut off filter (λ ≥ 400 nm) in a photochemical reactor under visible light. The TC initial concentration was 10 mg/L. A 0.10 g amount of photocatalysts was put into 100 mL of TC solution. Before the photodegradation experiment was initiated, the

suspension was magnetically stirred in the dark for 30 min to reach absorption equilibrium. The sampling analysis was conducted in a 10 min interval. The photocatalytic degradation ratio (DR) was calculated by the following formula:

$$DR = (1 - C_i / C_0) \times 100\%$$

C_0 is the initial absorbance of TC that reached absorption equilibrium, while C_i is the absorbance after the sampling analysis. The absorbance of TC was measured by a UV-vis spectrophotometer with the maximum absorption wavelength at 357 nm.

3. Results and discussion

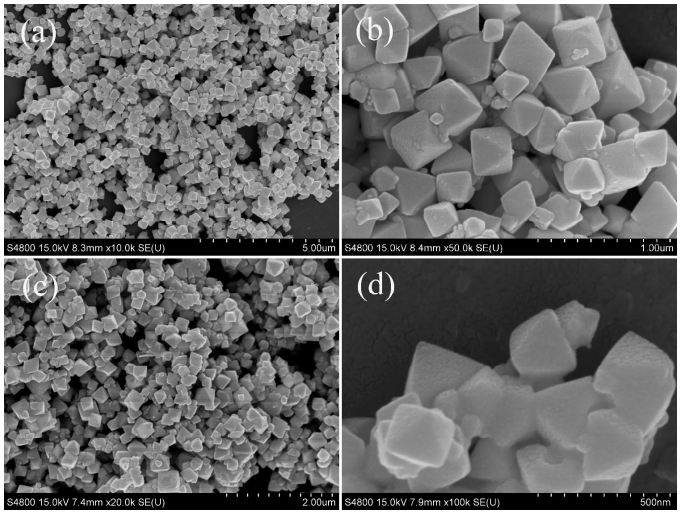

Figure 1. SEM images pattern in low-and high-magnification (left and right panels, respectively) of pure $Bi_{3.84}W_{0.16}O_{6.24}$ (a, b) and $Ag/Bi_{3.84}W_{0.16}O_{6.24}$ (c, d)

Figure 1 shows the SEM images of pure $Bi_{3.84}W_{0.16}O_{6.24}$ nanooctahedrons and $Ag/Bi_{3.84}W_{0.16}O_{6.24}$ composite nanooctahedrons. In the low-magnified SEM image (Figure 1a),

octahedral morphology of the products can be clearly observed. According to the high-magnification image (Figure 1b), the side length of a single $Bi_{3.84}W_{0.16}O_{6.24}$ octahedral nano-bulk is about 300-400 nm, the size and surface of $Bi_{3.84}W_{0.16}O_{6.24}$ nanooctahedrons are uniform and smooth. Compared with pure $Bi_{3.84}W_{0.16}O_{6.24}$ morphologies, the morphology of $Ag/Bi_{3.84}W_{0.16}O_{6.24}$ composite nanooctahedrons have not changed obviously, but the surface of the $Bi_{3.84}W_{0.16}O_{6.24}$ nanooctahedrons became rough and uneven after Ag nanopaticles loaded on. Figure 1d does not clearly represent the existence of Ag particles, which may have been due to the small amount of Ag.

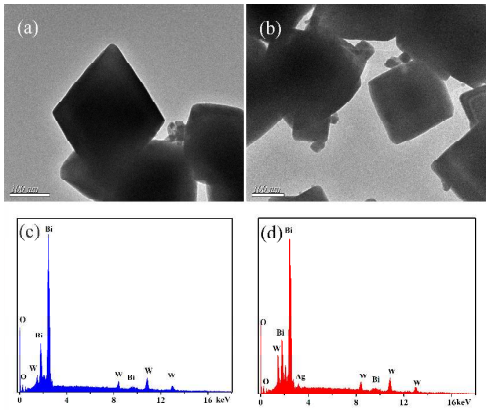

Figure 2. TEM and EDX microanalysis spectra of $Bi_{3.84}W_{0.16}O_{6.24}$ (a, c) and $Ag/Bi_{3.84}W_{0.16}O_{6.24}$ (b, d)

The morphology and microstructures comparison of $Bi_{3.84}W_{0.16}O_{6.24}$ nanooctahedrons and $Ag/Bi_{3.84}W_{0.16}O_{6.24}$ nanooctahedrons were further investigated by transmission electron microscopy (TEM) analysis. Figure 2a shows the TEM of pure $Bi_{3.84}W_{0.16}O_{6.24}$ samples, indicating the formation of octahedral nanostructure. A TEM image of $Ag/Bi_{3.84}W_{0.16}O_{6.24}$ nanooctahedrons samples is shown in Figure 2b. It's clearly observed that dark nanoparticles with the diameter of 10-20 nm circles distribution around the nanooctahedrons. In order to further confirm the existence of Ag, the areas with or without the deposited Ag were selected respectively for the energy-dispersed X-ray (EDX)

microanalysis. Compared Figure 2c and 2d, further confirmed the signal corresponding to silver was detected in the area with silver deposited.

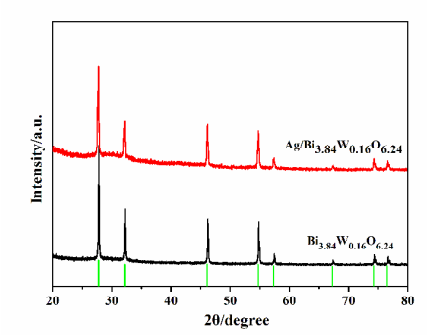

Figure 3. XRD patterns of $Bi_{3.84}W_{0.16}O_{6.24}$ and $Ag/Bi_{3.84}W_{0.16}O_{6.24}$ composite samples

The phase structure of the as-obtained products was examined by XRD pattern, as shown in Figure 3. It is observed that all samples exhibit specific diffraction peaks corresponding to an orthorhombic $Bi_{3.84}W_{0.16}O_{6.24}$ crystal phase (JCPDS no. 43-0447, the lattice constants of constants of $Bi_{3.84}W_{0.16}O_{6.24}$ crystal are a = 5.57 Å, b = 5.57 Å, and c= 5.56 Å.) and this indicates that the sample $Bi_{3.84}W_{0.16}O_{6.24}$ crystal synthesized by a facile microwave method has a high crystallinity. No other diffraction peak attributed to Ag is detected in the patterns, because the content of Ag is below the detection limit. Moreover, it is found that the intensities of diffraction peaks and crystallinity of the $Ag/Bi_{3.84}W_{0.16}O_{6.24}$ nanooctahedrons samples decreased compared with pure $Bi_{3.84}W_{0.16}O_{6.24}$, possibility due to Ag nanoparticles dispersed on the surface of the $Bi_{3.84}W_{0.16}O_{6.24,}$ which made surface of the $Bi_{3.84}W_{0.16}O_{6.24}$ nanooctahedrons became uneven and results in a low crystallinity.

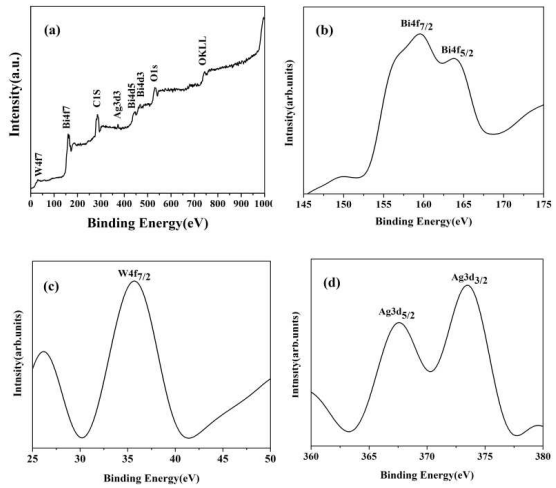

Figure 4. (a) The complete XPS spectra of $Ag/Bi_{3.84}W_{0.16}O_{6.24}$ composite samples; the resolution spectra of the etched samples for the elements of (b) Bi; (c) W; (d) Ag.

The surface composition and elementary oxidation states of the as-prepared $Ag/Bi_{3.84}W_{0.16}O_{6.24}$ sample with molar ratios R = 0.1 was investigated using XPS analysis. The corresponding experiment results are shown in Figure 4. The overall XPS spectrum shown in Figure 4(a) indicates that all of the peaks on the curve are ascribed to Bi, W, O, Ag and C elements and no peaks of other elements were observed. The presence of C comes mainly from carbon tape used for XPS measurement. Parts b-d in Figure 4 display the high-resolution spectrum for Bi, W and Ag species. According to Figure 4(b), the binding energies of Bi 4f7/2 and Bi 4f5/2 are 159.9 eV and 163.8 eV , respectively, which correspond to the characteristic peak of Bi^{3+}.The two peaks at the W region of 36.8 and 34.9eV can be assigned to the binding energy of W 4f (Figure 4c). Figure 4d shows the two characteristic peaks centered at 373.5 eV and 367.6 eV of Ag $3d_{5/2}$ and Ag $3d_{3/2}$. XPS peaks corresponding to Ag^{+} ion are not found. This result suggests the presence of metallic silver deposited on the $Bi_{3.84}W_{0.16}O_{6.24}$ octahedrons, did not react with $Bi_{3.84}W_{0.16}O_{6.24}$.

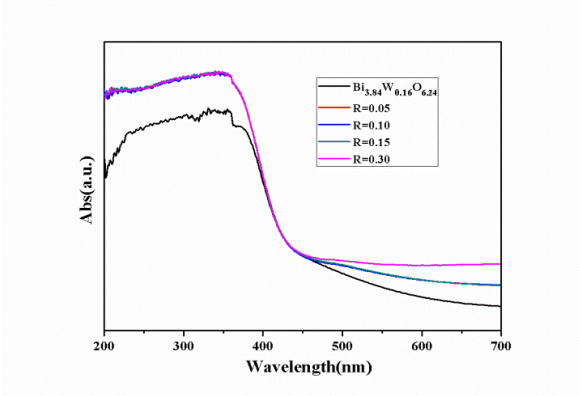

Figure 5. The UV-Vis absorption spectra of the pure $Bi_{3.84}W_{0.16}O_{6.24}$ and $Ag/Bi_{3.84}W_{0.16}O_{6.24}$ composites samples prepared molar ratios R =0.05, 0.1, 0.15, 0.3

The optical absorption properties of the as-prepared samples were investigated by a UV-vis spectrophotometer. The typical UV-vis diffuse reflection spectra of all samples show absorption bands with a steep edge in the visible light region observed as shown Figure 5. The prepared $Bi_{3.84}W_{0.16}O_{6.24}$ nanooctahedrons have a strong absorption at *ca.* 450 nm, and the $Ag/Bi_{3.84}W_{0.16}O_{6.24}$ nanooctahedrons show similar absorption spectra. However, it should be noted that $Ag/Bi_{3.84}W_{0.16}O_{6.24}$ nanooctahedrons obviously show an enhanced photo-absorption property in the visible light region after 450 nm compared with pure $Bi_{3.84}W_{0.16}O_{6.24}$. The prominent absorption in the visible light region could be attributed to the surface plasmon resonance band of Ag nanoparticles.[40-42] The SPR effect of Ag nanopaticles may make a partial contribution to the photocatalytic activity of $Bi_{3.84}W_{0.16}O_{6.24}$.

Photocatalytic activity and photoelectrochemical performance

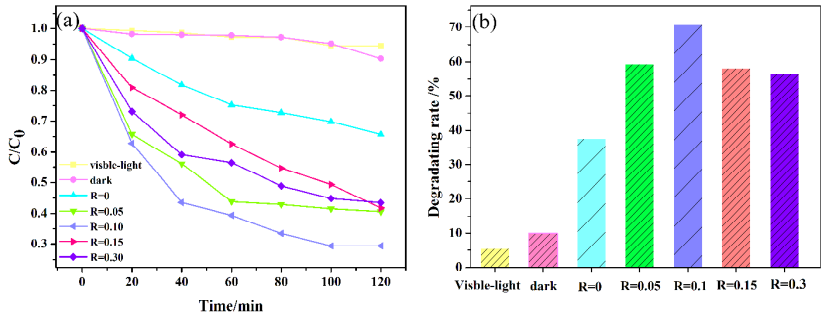

Figure 6. Typical plot for comparision of change in concentration vs irradiation time in presence of $Bi_{3.84}W_{0.16}O_{6.24}$ and various R of $Ag/Bi_{3.84}W_{0.16}O_{6.24}$

Photocatalytic performances of the pure $Bi_{3.84}W_{0.16}O_{6.24}$ nanooctahedrons and $Ag/Bi_{3.84}W_{0.16}O_{6.24}$ composite photocatalyst with different contents of Ag were comparatively evaluated from measuring the degradation efficiency of TC aqueous solution under visible light irradiation. The TC with the absence of photocatalysts did not degrade obvious before and after the visible light illumination for 120 min, which indicated TC was quite stable under the condition of visible-light irradiation. The TC with pure $Bi_{3.84}W_{0.16}O_{6.24}$ nanooctahedrons in the dark decreased at a low level due to the adsorption of the photocatalysts. In order further investigate the effect of Ag nanoparticles, the photocatalytic performance of the pure $Bi_{3.84}W_{0.16}O_{6.24}$ nanooctahedrons was also checked under the identical condition as that of $Ag/Bi_{3.84}W_{0.16}O_{6.24}$ composite nanooctahedrons. As shown in Figure 6, after 120 min visible light irradiation, TC degradation rate for pure $Bi_{3.84}W_{0.16}O_{6.24}$ nanooctahedrons can only approach 34.29%. These results suggested $Bi_{3.84}W_{0.16}O_{6.24}$ nanooctahedrons did not show much higher activity in the degradation of TC. However, it found that $Ag/Bi_{3.84}W_{0.16}O_{6.24}$ nanooctahedrons can notably enhance much photocatalytic activity in the degradation of TC when the Ag content is relatively lower, even eliminating the contribution of degradation effect brought by silver metal than bare $Bi_{3.84}W_{0.16}O_{6.24}$ obviously, which indicated that

TC could be degraded more efficiently by Ag/$Bi_{3.84}W_{0.16}O_{6.24}$ nanooctahedrons than $Bi_{3.84}W_{0.16}O_{6.24}$. Of particular concern, when the Ag content molar ratio is R = 0.1, Ag/$Bi_{3.84}W_{0.16}O_{6.24}$ composite photocatalyst exhibited the highest photocatalytic degradation efficiency. The photocatalytic activity of Ag loaded $Bi_{3.84}W_{0.16}O_{6.24}$ composite nanooctahedrons increased with the increasing of Ag content. But the photocatalytic activity decreased at the higher Ag content. That is to say there is an optimum loading level of Ag content. It is possible because the excessive Ag led to $Bi_{3.84}W_{0.16}O_{6.24}$ nanooctahedrons being covered, which causes the reduction of contact area between $Bi_{3.84}W_{0.16}O_{6.24}$ nanooctahedrons and water.

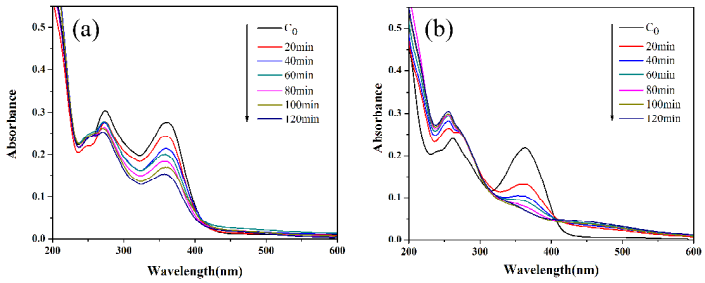

Figure 7. Time-dependent absorption spectra of TC (a) $Bi_{3.84}W_{0.16}O_{6.24}$; (b) Ag/$Bi_{3.84}W_{0.16}O_{6.24}$

Figure 7 shows a comparison of photocatalytic performances of $Bi_{3.84}W_{0.16}O_{6.24}$ nanooctahedrons and Ag/$Bi_{3.84}W_{0.16}O_{6.24}$ nanooctahedrons samples for degradation of TC. It can be seen that variation of absorption total concentration of TC are monitored by examining the maximum absorption in UV-vis spectra at 357 nm due to the narrow range of molar extinction coefficient. Compared Figure 7a and Figure 7b, it can be obviously noticed TC with R = 0.1 Ag/$Bi_{3.84}W_{0.16}O_{6.24}$ nanooctahedrons decreased higher than pure $Bi_{3.84}W_{0.16}O_{6.24}$ sample. Particularly, from Figure 7b we can be observed that the characteristic absorption peak of TC at 357 nm decreases successively with increasing visible light irradiation time and disappears within 40 min. The above results indicate the

enhanced that as-prepared $Ag/Bi_{3.84}W_{0.16}O_{6.24}$ nanooctahedrons composites exhibit high photocatalytic activity for degradation of TC.

4. Mechanism of Enhanced Photoactivities

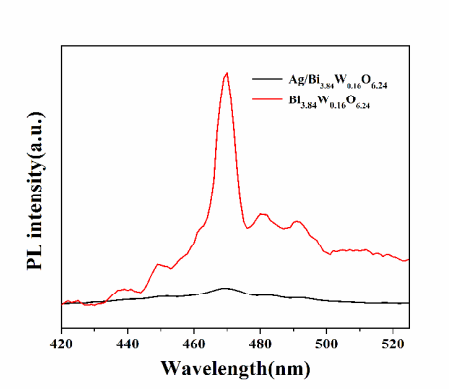

Figure 8. PL emission spectra of different samples at an excitation wavelength of 320 nm

In order to better understand the photocatalytic process of the degradation of TC mechanism, photoluminescence (PL) were conducted on different samples. The photoluminescence spectra of solid samples were recorded over the wavelength range 420-520 nm with the excitation at 320 nm, both samples exhibited the usual band-edge emission with peak at 470 nm. It could be seen from photoluminescence spectra that there was a significant decrease in the intensity of PL spectra of $Ag/Bi_{3.84}W_{0.16}O_{6.24}$ composite photocatalyst. It is well acknowledged that the PL emission intensity of a semiconductor is proportional to the opportunity of the recombination of photoinduced electron-hole pairs.[43] Consequently, lower PL emission intensity of $Ag/Bi_{3.84}W_{0.16}O_{6.24}$ nanooctahedrons suggests Ag nanoparticles can easily capture the photoexcited electrons from $Bi_{3.84}W_{0.16}O_{6.24}$ and promote interfacial charge transfer, resulting in lower recombination rate of e^-/h^+pairs.

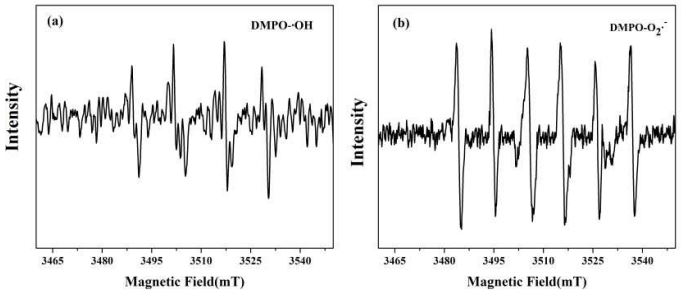

Figure 9. ESR spectra of radical adducts trapped by DMPO in Ag/ $Bi_{3.84}W_{0.16}O_{6.24}$: (a) DMPO-OH formed in irradiated aqueous dispersions; (b) DMPO-O_2^- formed in irradiated methanol dispersions

To further investigate the reactive species evolved during the photocatalytic reaction process, such as hydroxyl radical and superoxide radical species, we tested the electron spin resonance (ESR) with DMPO technique. 10 mg R = 0.1 Ag/ $Bi_{3.84}W_{0.16}O_{6.24}$ nanooctahedrons and 40 μL DMPO were dissolved in 0.5 mL deionized water and stirred for 5 min (solution A); solution B was prepared in the same manner except that water was replaced by CH_3OH. Solution A was used for the detection of hydroxyl radicals (DMPO- • OH), and solution B was used for the detection of superoxide radicals (DMPO- • O_2^-) and the results were shown in Figure 9. From Figure 9a, we found four characteristic peaks with relative intensities of 1:2:2:1 from the DMPO- • OH adducts were detected during the reaction process, suggesting that hydroxyl radicals were formed in the catalytic reaction. Similarly, from Figure 9b, ESR signals of DMPO- • O_2^- adducts with characteristic six characteristic peaks are also observed with visible-light-irradiated methanol dispersions.[44-46] Therefore, on the basic of the ESR results, we can confirm presence of • OH and • O_2^-.

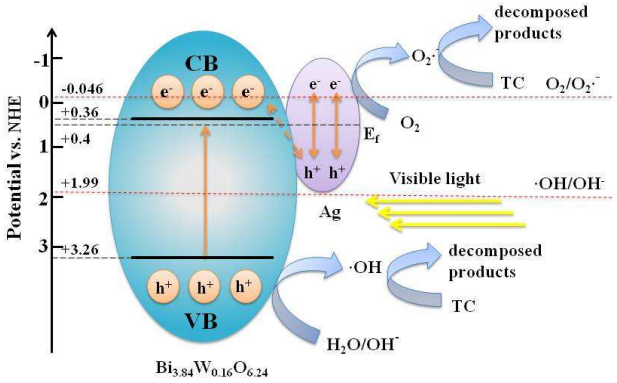

Scheme 1. Mechanistic Pathway of Electrons and Holes under Visible Light Illumination on $Ag/Bi_{3.84}W_{0.16}O_{6.24}$ Photocatalysts

On the basis of the experimental results and the literature, a possible mechanism of the photocatalytic process of TC degradation using of $Ag/Bi_{3.84}W_{0.16}O_{6.24}$ composite photocatalyst can be estimated and be shown as in Scheme 1. $Bi_{3.84}W_{0.16}O_{6.24}$ sample shows visible-light phtocalytic activity as it can absorb visible-light to *ca.*450 nm according to its UV-vis spectrum in Figure 5. When subjected to visible-light irradiation, the photogenerated electrons were excited to the conduction band of $Bi_{3.84}W_{0.16}O_{6.24}$ with holes left in the valence under visible light irradiation. $Bi_{3.84}W_{0.16}O_{6.24}$, as another complex oxide of bismuth tungsten oxide, should have a band structure similar to that of Bi_2WO_6. It is well-known that the CB and VB level of Bi_2WO_6 are *ca.* +0.36 and +3.26 V(*vs* NHE)[47]. Therefore, it can be deduced that the VB holes of $Bi_{3.84}W_{0.16}O_{6.24}$ have a strong oxidation power due to its high potential (+3.26 V *vs* NHE). Meanwhile, VB potential of $Bi_{3.84}W_{0.16}O_{6.24}$ is more negative than the standard redox potential of OH^-/ • OH(1.99 V *vs* NHE)[48], therefore h_{VB}+ can oxidize OH^- to generate •OH radicals directly in $Bi_{3.84}W_{0.16}O_{6.24}$ photocatalytic system. These as-produced • OH radicals can then degrade the TC molecules into CO_2 and H_2O.

On the other hand, because of the surface plasmonic resonance effect and dipolar character of metallic Ag, metallic Ag can also absorb visible light, and the absorbed photon would be efficiently separated to an electron and a hole.[49-51] When subjected to visible-light irradiation, the surface Ag nanoparticles function as visible-light-harvesting and electron-generating centers owing to the strong surface plasmon resonance (SPR). The photogenerated electrons of $Bi_{3.84}W_{0.16}O_{6.24}$ transfer to the Ag nanoparticles to recombine with the plasmon-induced holes produced by plasmonic absorption of Ag nanoparticles. [52-55] Ag nanoparticles entrap electrons and reduced the recombination possibility with photogenerated holes of $Bi_{3.84}W_{0.16}O_{6.24}$. As a result, more holes will have opportunity to participate in the oxidation reactions on the surface reacted with water and OH^- to produce • OH radicals. More photoexcited carriers can be generated, giving a positive influence on the photocatalytic activity of the heterostructured $Ag/Bi_{3.84}W_{0.16}O_{6.24}$. Meanwhile, the increased electron density lifts the Fermi energy level of Ag shifts from 0.4 V (vs. NHE) to the energy level higher than the standard redox potential of $O_2/•O_2^-$ (–0.046 V vs. NHE), [40] leading to a reserved reduction ability of $e_{CB}^-$for the formation of $•O_2^-$radicals and further oxidize TC to decomposed products. Therefore, compared with the $Bi_{3.84}W_{0.16}O_{6.24}$, it is clear that the $Ag/ Bi_{3.84}W_{0.16}O_{6.24}$ have a strong photocatalytic activity. The high-efficiency photocatalytic activity of the as-prepared $Ag/Bi_{3.84}W_{0.16}O_{6.24}$ can be ascribed the SPR absorption of silver nanoparticles as well as fast generation, separation and transportation of the photogenerated carriers.

Stability and Reusability of $Ag/Bi_{3.84}W_{0.16}O_{6.24}$

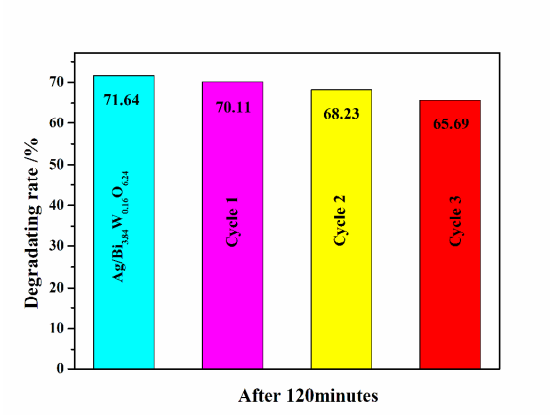

Figure 10. Cycle runs in the photocatalytic degradation of TC by $Ag/Bi_{3.84}W_{0.16}O_{6.24}$ under visible-light illumination

The possibility of catalyst reuse and stability is of paramount importance for the catalyst in photocatalytic processes, since it could contribute significantly to lowering the operational cost of the process. Therefore, three consecutive cyclic photodegradation experiments were performed for $Ag/Bi_{3.84}W_{0.16}O_{6.24}$, each time using the same catalyst and a fresh TC solution. The results of the cycling experiments of the $Ag/Bi_{3.84}W_{0.16}O_{6.24}$ composite photocatalyst for photodegradation of TC under visible-light irradiation are depicted in Figure 10, a trivial decline (~6%) in photocatalytic activity after three cycles, which could result from the unavoidable loss of the sample during recycling. The catalysts were monitored by using SEM, TEM and X-ray diffraction and the results shown in Supporting Information. It indicates that the $Ag/Bi_{3.84}W_{0.16}O_{6.24}$ nanooctahedrons have high stability during the photocatalytic degradation.

4. CONCLUSIONS

Noble metal Ag was deposited on $Bi_{3.84}W_{0.16}O_{6.24}$ has been successfully synthesized via a versatile and facile microwave method. Furthermore, the photocatalytic degradation of TC under

visible-light is conducted to investigate the effect of Ag. The photocatalytic activity of Ag/$Bi_{3.84}W_{0.16}O_{6.24}$ composite photocatalyst was greatly enhanced compared with pure $Bi_{3.84}W_{0.16}O_{6.24}$. The content of silver has an impact on the catalytic activity of Ag/ $Bi_{3.84}W_{0.16}O_{6.24}$ composites photocatalyst. The active species $\bullet O_2^-$ and •OH radicals were detected by ESR technology and proved to be the most important reason for the photodegradation of TC. Synergetic effect of the noble metal and semiconductor is important for improving the performance of nanocomposites in photocatalytic applications. This work is helpful for the design of new photocatalysts with enhanced photocatalytic activity, meanwhile provide a new insight into the fabrication of plasmonic photocatalysts with high performance.

Acknowledgements:

We gratefully acknowledge the financial support of the National Natural Science Foundation of China (21276116, 21477050, 21301076 and 21303074), Excellent Youth Foundation of Jiangsu Scientific Committee (BK20140011), Program for high-level innovative and entrepreneurial talents in Jiangsu Province, Program for New Century Excellent Talents in University (NCET-13-0835), Henry Fok Education Foundation (141068) and Six Talents Peak Project in Jiangsu Province (XCL-025), the Reasearch of Cyanobacteria Bloom-forming Mechanism in Eutrophic Lake Taihu and Algal Inhibitation and Removal Technology in Situ (CZ20140017).

References:

[1] R. Li., Y. Zhang, C.C. Lee, L. Liu and Y. Huan, *J. Sep. Sci.*, 2011,34,1508.

[2] R. Wei, F. Ge, S. Huang, M. Chen and R. Wang, *Chemosphere,* 2011,82,1408.

[3] J. J. Lo´pez Pen˜alver, C.V. Go´mez Pacheco, M. Sa´nchez Polo and J.R. Utrilla. *J Chemt. Technol. Biot.* 2012, 88, 1096.

[4] X.J. Ding, and S.F. Mou, *J Chromatogr. A*, 2000, 897, 205.

[5] A. Onal, *Food Chem.*, 2011,127, 197.

[6] V.F. Samanidou, K.I. Nikolaidou, and I.N. Papadoyannis, *J Sep Sci,.* 2007, 30, 2430.

[7] V. Belgiorno, L. Rizzo , D. Fatta , Della Rocca, C., Lofrano, G.,Nikolaou, A., Naddeo, V., and Meric, S., *Desalination*, 2007, 215, 166.

[8] R. D. F. P. M. Moreira, T. P. Sauer, L. Casaril, and E. Humeres, *J. Appl. Electrochem.* 2005, 35, 821.

[9] J. Shi, J. Zheng, P. Wu, and X. Ji, *Catal. Commun*. 2008, 9, 1846.

[10] T. J. Yan, X. Y. Yan, R. R. Guo, W. N. Zhang, W. J. Li, and J. M. You, *Catal. Commun.*, 2013,42, 30.

[11] C. Belver, C. Adán, M. Fernández-García, *Catal. Today* , 2009, 143, 274.

[12] L. Rizzo , *J. Hazard. Mater*. 2009,165, 48.

[13] H. Wang, J. Li, X. Quan, and Y. Wu, *Appl. Catal. B,* 2008, 83, 72.

[14] C. M. Li, G. Chen, J.X. Sun, Y. J. Feng, J. J. Li , and H. J. Dong, *Appl. Catal. B Environ.*, 2015, 163, 415.

[15] G. Zhao, S. Liu, Q. Lu, H. Sun, *J. Alloy. Compd*., 2013, 578, 12.

[16] C. M. Li , G. Chen, J. G. Sun, H.J. Dong, Y. Wang, and C.D. Lv, *Appl. Catal. B Environ.,* 2014, 161, 383.

[17] A. P. Finlayson, E. Ward, V.N. Tsaneva, and B.A. Glowacki, *J. Power Sources*, 2005,145, 667.

[18] Y. Zhou, K. Vuille, Andre Heel,and Greta R. Patzke, *Z. Anorg. Allg. Chem.*, 2009, 635, 1848.

[19] Y. Yan, Y. Wu, Y. Yan, W. Guan, and W. Shi, *J. Phys. Chem.c.*, 2013,117, 20017..

[20] G. Y. Zhang, Y. Feng, Q. S. Wu, Y. Y. Xu, and D. Z. Gao, *Materials Research Bulletin, 2012*,47,1919.

[21] S.S. Yao, J.Y. Wei, B.B. Huang, S.Y. Feng, X.Y. Zhang, Y. Qin, P. Wang, Z.Y. Wang, Q.Zhang, X.Y. Jing, and J. Zhan, *J. Solid State Chem.*, 2009,182, 236.

[22] C.Y. Wang, L. Y. Zhu, C. Song, G. Q. Shan, and P. Chen, *Appl. Catal. B Environ.*,2011, 105, 229.

[23] W.S. Guan, Y. F. Wu, and S.F. Sun, *Fresen. Environ. Bull.*, 2014, 23, 769.

[24] E.S. Aazam, *J. Ind. Eng. Chem.*, 2014, 20, 4008.

[25] Juliana Ferreira de Brito, Alexander Alves da Silva, Alberto José Cavalheiro and Maria Valnice Boldrin Zanoni, *Int. J. Electrochem. Sci.*, 2014, 9, 5961.

[26]R. M. Mohamed, E. S. Baeissa, *J. Ind. Eng. Chem.*, 2014, 20, 1367.

[27]H. Yu, R. Liu, X. Wang, P. Wang, J. Yu, *Appl. Catal. B*, 2012, 326, 111.

[28]X. Li, R. Huang , Y. Hu, Y. Chen, W. Liu , R. Yuan , Z. Li ,*Inorg. Chem.*, 2012, 51, 6245.

[29]L. Yu , Y. Huang , G. Xiao and D. Li, *J. Mater. Chem. A*,2013, 1, 9637.

[30] S. Karlsson, J. Boixel, Y. Pellegrin, E. Blart, H.-C. Becker, F. Odobel and L. Hammarstrom, *J. Am. Chem. Soc.*, 2010, 132, 17977.

[31] R.C. Liu, *J. Phys. Chem. C* 2009, 113, 9368.

[32] V. Subramanian, E. E. Wolf, and P. V. Kamat, *J. Am. Chem. Soc*.,2004, 126,4943.

[33] W. Zhao, Y.Guo, Y. Faiz, T. Y. Wen, C, Sun, S,M, Wang,Y,H. Deng, Y. Zhuang, Y.Li, X.M. Wang, H.He, and S.G. Yang, *Appl. Catal. B Environ.*, 2015, 163, 288

[34] W.X. Zhang, X.N. Yang, Q. Zhu, K.Wang, J.B. Lu, M. Chen, and Z.H. Yang, *Ind.Eng.Chem.Res*., 2014, 53, 16316.

[35] Y. H. Ao, J.L. Xu, Y.Y. Gao, P.F. Wang, C. Wang , J. Hou, and J. Qian, *Catal.Commun.*,2014, 53, 21.

[36] C. C. Han, L. Ge, C.F. Chen, Y. J. Li, Z. Zhao, X. L. Xiao, Z. L. Li and J. L. Zhang, *J. Mater. Chem. A,* 2014, 2, 12594.

[37] S. Kuriakose1, V.Choudhary, B.Satpati and S.Mohapatra, *Beilstein J. Nanotechnol.*, 2014, 5, 639.

[38] X. J. Bai, R.L. Zong, C. X. Li, D. Liu, Y. F. Liu, Y. F. Zhu, *Appl. Catal. B Environ.,* 2014, 147, 82.

[39] H. J. Cheng, J. G. Hou, H. M. Zhu and X. M. Guo, *Rsc. Adv.*, 2014, 78, 41622.

[40] J.B. Zhou, Y. Cheng, and J.G. Yu, *J. Photoch. Photobio. A*, 2013, 233, 82.

[41] L. Sun, R. Z. Zhang, Y. Wang, W. Chen, *Appl. Mater. Interfaces*, 2014, 6, 14819.

[41] D. Keith Roper, W. Ahn, and M. Hoepfner, *J. Phys. Chem. C*, 2007, 111, 3636.

[43] G. H. Zhang, W. S. Guan, H. Shen, X. Zhang, W. Q. Fan, C. Y. Lu, H. Y. Bai, L. S. Xiao, G. Wei, and W.D. Shi, *Ind. Eng. Chem.Res*., 2014,54,5443.

[44] W. R. Zhao, Y. Wang, Y. Yang, J. Tang and Y.N. Yang, *Appl. Catal. B Environ*., 2012, 115, 90.

[45] J. J. Sun, X. Y. Li, Q. D. Zhao, J. Ke, and D. K. Zhang，*J. Phys. Chem.c.*, 2014, 118, 10113.

[46] Y. Y. Yao, L. Wang, L. J. Sun, S. Zhu, Z. F. Huang, Y. J. Mao, W. Y. Lu and W. X. Chen，*Chem. Eng. Sci.*，2013，101, 424.

[47] X. N. Li, R. K. Huang, Y. H. Hu, Y. J. Chen, W. J. Liu, R. S. Yuan, and Z.H. Li, Inorg. Chem. 2012, 51, 6245.

[48] Y. X. Yang , Y. N. Guo, F. Y. Liu , X. Yuan, Y. H. Guo, S. Q. Zhang , W. Guo, and M. X. Huo, *Appl. Catal. B Environ*., 2013, 142, 828.

[48] J. G. Hou, Z. Wang, C. Yang, W. L. Zhou, S. Q. Jiao, and H. M. Zhu, *J. Phys. Chem.C.*, 2013, 117, 5132.

[50] J. G. Hou, C. Yang, Z. Wang, Q. H. Ji, Y. T. Li, G. C. Huang, S. Q. Jiao and H. M. Zhu, *Appl. Catal. B Environ*., 2013, 142, 579.

[51] X. F. Wang, S. F. Li, Y. Q. Ma, H. G. Yu, and J.G. Yu, *J. Phys. Chem.C.*, 2011, 115, 14648.

[52] J. Ren, W.Z Wang, S.M. i Sun, L. Zhang, and J. Chang, *Appl. Catal. B Environ*., 2009, 92, 50.

[53] J.Q. Li, Z. Y. Guo, and Z.F. Zhu, *Ceram. Int.*2014, 40, 6495.

[54] H.L. Wang, L.S. Zhang, Z.G. Chen, J.Q. Hu, S.J. Li, Z.H. Wang, J.S. Liu and X.C. Wang, *Chem. Soc. Rev.*, 2014, 43, 5234.

[55] Y.N. Guo, L. Chen, F.Y. Ma, S.Q. Zhang, Y.X. Yang , X. Yuan, andY. H. Guo, *J. Hazard. Mater.*, 2011, 189, 614.